P H Y S I C A L   R E V I E W   L E T T E R S

Droplet Traffic in Microfluidic Networks: A Simple Model for Understanding and Designing

Michael Schindler and Armand Ajdari

Laboratoire PCT, UMR "Gulliver" CNRS-ESPCI 7083, 10 rue Vauquelin, 75231 Paris cedex 05, France
(Received 16 July 2007; published 28 January 2008)

We propose a simple model to analyze the traffic of droplets in microfluidic "dual networks." Such functional networks which consist of two types of channels, namely, those accessible or forbidden to droplets, often display a complex behavior characteristic of dynamical systems. By focusing on three recently proposed configurations, we offer an explanation for their remarkable behavior. Additionally, the model allows us to predict the behavior in different parameter regimes. A verification will clarify fundamental issues, such as the network symmetry, the role of the driving conditions, and of the occurrence of reversible behavior. The model lends itself to a fast numerical implementation, thus can help designing devices, identifying parameter windows where the behavior is sufficiently robust for a device to be practically useful, and exploring new functionalities.

Injecting immiscible fluids into a microfluidic system has been found to permit the controlled generation of droplets or bubbles [1]. Rapidly, *droplet microfluidics* has developed beyond early observations because of its promises for a diversity of fields [2,3]: studies of chemical kinetics and time-controlled synthesis [4], high-throughput screening [5], fabrication of remarkable colloidal objects [6], combinatorial chemistry [4], and even nonelectronic coding or computing functions [7,8]. These tasks require mastering the generation of droplets, their traffic in potentially complex networks, and sometimes their splitting or merging. One can either employ passive means by relying on hydrodynamics and capillarity alone [1,2,4,6,7], or integrate active actuators (electric, dielectric, pneumatic) in the devices [2,9]. Difficulties often arise even in simple geometries if the complex behavior of dynamical systems (period doubling, chaotic behavior, etc.) occurs [9,10].

We here focus on the traffic of droplets only, without splitting or merging, in what we name *dual networks*, i.e., networks combining channels that can be accessed by droplets (*transport channels*) and others that cannot (*"bypass" channels*); see Fig. 1. This family of networks encompasses many recently proposed solutions [7,8,11,12]. Building on recent works [11,13], we introduce a simple numerical tool to analyze the collective motion of droplets in such a dual network. We show this tool to be powerful in both illuminating fundamentals ruling the traffic (including considerations of symmetry and reversibility) and as a means to predict the capability and robustness of a given design in performing a given function. In particular, we illustrate these ideas by analyzing three recently proposed devices as displayed in Fig. 1: a reversible encoding loop [8] [1(a)], a ladder for synchronizing droplets between parallel channels [7] [1(b)], and a bypassed T junction for symmetric splitting of a droplet train [12] [1(c)].

Simple model.—We model both the flow of the continuous phase and the traffic of droplets in an arbitrary *dual*

network of transport channels and bypasses, represented as a simple directed graph of nodes and links as in Fig. 1. The instantaneous flow state is given by a pressure P_α at each node and a total flow rate Q_i in each channel. These variables are related by equations similar to Kirchhoff's rules for electrical circuits. Mass conservation at node α, taking into account a possible external injection $Q_{\text{ext}}^{(\alpha)}$, reads

$$\sum_{i \text{ connected to } \alpha} \epsilon_i Q_i = Q_{\text{ext}}^{(\alpha)}, \tag{1}$$

where $\epsilon_i = \pm 1$ account for the orientation of the link. In channel i the flow rate Q_i is related to the pressure difference between its two end nodes $\alpha_{\text{in}(i)}$ and $\alpha_{\text{out}(i)}$,

$$\Delta P_i = P_{\alpha_{\text{in}(i)}} - P_{\alpha_{\text{out}(i)}} = R_i Q_i. \tag{2}$$

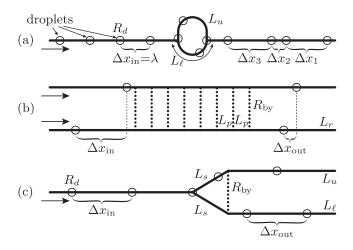Equation (2) defines the *hydrodynamic resistance* R_i of

FIG. 1. Graph representations of three recently proposed dual networks: (a) a loop [7]; (b) a ladder [8]; (c) a bypassed T junction [12]. Full and dotted lines correspond to transport channels (accessible to droplets) and bypass channels (forbidden to droplets). Droplets are indicated by circles.

channel i. For flows without droplets at low Reynolds number it reduces to a constant value $\bar{R}_i$, proportional to the viscosity and to the channel length L_i: $\bar{R}_i \propto L_i$.

Droplets or bubbles in the channel significantly modify the picture in a quite complex way [3,11,13]. A simplification occurs if the droplets are sufficiently distant from one another (typically a few channel diameters away) so that their flow perturbations do not interact. In the mentioned experiments the ratio of distance to diameter is approximately 10 (loop and ladder) and 5 (bypass junction). Each droplet then yields an additive increment R_d to the resistance. In this Letter, we make the further simplification that all droplets are equal and so are the cross sections S of the channels transporting droplets (these restrictions can be easily lifted in the numerical model), so that for n_i droplets in channel i,

$$R_i = \bar{R}_i + n_i R_d. \tag{3}$$

Identical droplets with no interaction move all at the same velocity v_i in a channel with a given flow rate Q_i, which we write with a proportionality factor β/S,

$$v_i = \beta Q_i / S. \tag{4}$$

In general, both R_d and β will vary with Q_i [13,14]. The simplifications in (3) and (4), however, have proved to hold in experimental realizations [11].

The flow state, consisting of all pressure and flow rate values, is uniquely determined by the set of linear Eqs. (1) and (2) when complemented by appropriate boundary conditions at the end nodes, i.e., specification of either the pressure or the externally injected flow rate. An important point is that this flow state persists until a droplet arrives at a node and enters another channel, thereby modifying the set of resistances. To describe droplet traffic, we thus track the locus of the droplets (modeled as points) along the channels. When a droplet arrives at a node where there are several channels to choose from, a *selection rule* is required. We focus here on locally symmetric T junctions for which the droplets enter the channel with the instantaneous larger flow rate [11,13].

Altogether, we propose the following algorithm: (i) Compute the pressures and flow rates for a given set of droplet positions using Eqs. (1) and (2); (ii) determine the droplet velocities according to Eq. (4); (iii) determine the next time when either a droplet arrives at a junction or a new one is injected, and advance all droplets to this time; (iv) decide which route the triggering droplet takes, update the channel resistances of the affected channels, and return to step (i).

Clearly, step (iii) is the big time saver that allows fast computations of rather involved histories. This scheme can be straightforwardly adapted to networks with channels of different cross-sections and to other junction geometries, but the present version is sufficient to revisit recently proposed devices and discuss fundamental issues.

Reversibility.—Fuerstman *et al.* [8] presented a device that allows reversible "encoding" of information in inter-droplet distances: Two long channels, used to store droplet series, are connected by a slightly asymmetric loop [Fig. 1(a)]. A regular train of droplets, injected through one channel into the loop, exits the loop as a complex modulated sequence. The interdroplet distances result from the "decisions" taken by the droplets when entering either branch of the loop. Each decision is affected by the presence of previous droplets in the loop. The slight asymmetry of the loop gives rise to periods of $2, 3, \ldots, 7$ in the outgoing sequence, depending on the initial interdroplet distance [8]. When we apply our simple model using parameters reasonably related to those of the experimental realization, we do obtain a comparable cascade of periods (2, 3, 5, 7, 9, etc.), as a characteristics of dynamical systems at work in this network [15].

A remarkable result by Fuerstman *et al.* [8] is that upon reversal of the flow direction, the starting sequence of droplets is restored, i.e., the system exhibits *reversibility*. This is far from being obvious, keeping in mind that the selection rule is not intrinsically reversible.

To investigate the question of reversibility further, in our numerics we send a periodic train of droplets through the loop until N droplets have reached the other side, then invert the flow direction and send them back. The resulting $(N-1)$ interdroplet distances after this return trip through the loop are plotted in Fig. 2(a) for several values of the initial distance λ, ranging from 0 to the maximum for which two droplets interact, $\lambda_{\max} = L_\ell [1 + (\bar{R}_\ell + R_d)/\bar{R}_u]$ [see Fig. 1(a) for the parameters]. The most striking feature of Fig. 2(a) is that it predicts windows of values of λ for which the system behaves reversibly and other
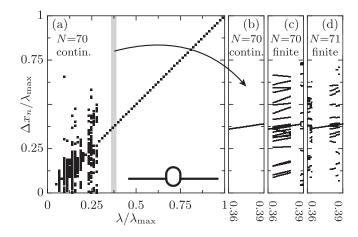

FIG. 2. Final distances Δx_n between 70 droplets after a return journey through the loop of the device in Fig. 1(a), as a function of the initial period λ. Reversibility is observed where all 69 symbols collapse on the diagonal, see also the zoomed panel b. The results differ for a finite droplet train (panels c and d), where also the number of droplets matters. The parameters $L_u/L_\ell = 1.112$, $R_d/\bar{R}_\ell = 1.5$, are compatible with data from Ref. [8] [15].

windows for which it does not (points not on the diagonal). It also sheds light on the importance of the precise conditions at flow inversion: For the same parameter interval [15], both full reversible behavior [Fig. 2(b)] and a complicated interrupted pattern [Fig. 2(c)] can be produced. In panels 2(a) and 2(b) the droplets were perpetually injected, such that the loop was not empty when changing the flow direction. Conversely, in Fig. 2(c) and 2(d), a finite train of N droplets was sent to and fro, with an empty loop in the meantime. This latter case is hardly reversible and depends on the precise number of droplets.

Let us underline that nonreversibility is deeply linked to the selection rule, and thus to the presence of junctions between transport channels. In a dual network with no such junctions, one expects the behavior to be reversible.

Reversibility and symmetry of the design.—This observation leads us to a rather generic point regarding the kind of functions that a fore-aft symmetric device can achieve if the dynamics is reversible. A good support for this discussion is the recently proposed [7] symmetric ladder network of Fig. 1(b). Two transport channels are connected by a few (narrower) bypass channels. The device has been shown to perform the following function: Two droplets arriving with a given delay in the entrance channels leave the system with a much reduced distance, allowing synchronization between the two channels. Why is this remarkable? On one hand, (A) as the device is symmetric in design, if distances are reduced going one way, they should also be reduced going the reverse way. On the other hand, (B) the absence of junctions leading to ''decision making steps'' implies reversible dynamics, so that if the distance decreases one way, it should increase the other way: Such paradoxical statements are commonly used in low Reynolds number fluid dynamics to show that there can be no net effect. Here, experiments tell us otherwise.

Running our model immediately resolves the paradox in a manner that is practically relevant: The function can be achieved only if the boundary conditions are not symmetric! For example, if we apply constant flow rates in the two entering arms and a fixed pressure at the two exiting nodes, we recover qualitatively the phenomenology described in Ref. [7] with distance reduction [see case (a) in Fig. 3]. This reduction is not forbidden by the symmetry argument, as changing the sign of the flow rates and of the pressures yields a pattern of boundary conditions that is not the symmetric image of the initial situation, eliminating argument (A). In this new situation [case (c) in Fig. 3] the ladder acts as a distance expander rather than a distance contractor, in accordance with (B). Conversely, if we use fixed pressures at all end nodes, then the effect vanishes, as required by the symmetry argument (A + B) above [case (b) in Fig. 3]. Our analysis thus clarifies the limits of use of this device as a synchronizing functional block in a network context.

At this stage, we have demonstrated that our model reproduces qualitatively and quantitatively the perform-
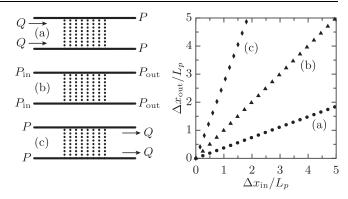

FIG. 3. Change of droplet misalignment in the ladder device. Only the boundary condition (a) leads to a contraction; fixed pressures on both ends (b) do not affect the offset, while it grows in (c). $R_d/\bar{R}_p = 20$, $R_{by}/\bar{R}_p = 5$, $L_r/L_p = 5$.

ance of existing devices. It illuminates the essential role of the imposed driving conditions [16], and it provides *a priori* indication as to the dynamic behavior (period doubling, reversibility, etc.) as a function of design parameters (geometrical symmetry) and operational parameters (droplets distance, etc.).

Designing Devices: Optimization and Robustness.—The speed of our numerical scheme permits fast optimization of identified designs. For example, we can scan the effect of different parameters of the ladder device [Fig. 3(a)], such as the number of bypasses, their resistance, their distance, or the resistance of the droplets. The parameter $R_d/\bar{R}_p$ has the strongest influence: the closer the bypasses, the better. Conversely, making the side arms of the transport channels (L_r) very long, has a negative effect on the contraction. Increasing the number of bypasses from 3 to 10, or making them 100 times less resistant only weakly improves the contraction result.

Beyond this optimization in an ideal world, an essential point for suggested designs to turn into efficient working devices is their robustness to both fabrication errors and operational variations—virtues that are rarely quantified. We demonstrate the easy use of our tool to qualify the bypassed T junction of Fig. 1(c), proposed in Ref. [12]. The aim of this engineered junction is to provide reliable alternation of the channel chosen by incoming droplets. How it works is detailed in Ref. [12]—in short, the bypass channel imposes similar pressures at both its ends. A droplet having chosen one route is then able to ''block'' its channel such that the next droplet favors the other one due to its larger flow rate. With our numerical scheme we immediately recover the same parameter window for which the experimental design has been shown to be successful [cf. Fig. 3 in Ref. [12]].

We can systematically explore the robustness of the alternating behavior to imperfections of the device. These may consist of a ''quenched'' design asymmetry, such as a small systematic bias in the decision rule or a difference in
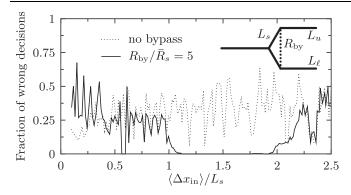
FIG. 4.   Fraction of wrong (not strictly alternating) decisions in
T junctions with and without bypass [Fig. 1(c)]. The interval
without errors around the average droplet distance $\langle \Delta x_{in} \rangle \approx$
$1.5L_s$ corresponds to the experimental findings in Fig. 3 of
Ref. [12]. The robustness of the behavior is challenged by an
asymmetry ($L_u/L_\ell = 1.01$) and a random perturbation of the
incoming distances (standard deviation is 5% of the average
value). $R_d/\bar{R}_s = 0.3$.

arm lengths; or they may come as random fluctuations in
the incoming droplet distance or in the pressures at the
outlets. Figure 4 shows the effect of a random Gaussian
perturbation of the incoming droplet distances, combined
with a slight asymmetry of the channel lengths behind the
bypass. Both perturbations lead to the complete failure of
an unbypassed junction, whereas even a thin bypass ro-
bustly yields a perfect alternation in a significant window
of parameters.

Playing with this analysis we find another remarkable
property of the bypassed T junction, namely, noise reduc-
tion in the droplet distances. The distances in the two
outgoing sequences have a smaller standard deviation
than the incoming train (data not shown). This effect
operates for a single junction and can be amplified by using
a cascade of several junctions, connected in such a way that
the average hydrodynamic resistances are balanced at each
stage of the cascade [17]. At each level of the cascade the
noise is reduced because the relative standard deviation of
the distance between over-next droplets is only $1/\sqrt{2}$ times
that between adjacent droplets.

Conclusion.—We have proposed a simple yet efficient
fast numerical tool to analyze the traffic of droplets in
"dual microfluidic" networks. Through an analysis of
three recently proposed devices, we have shown the power
of this tool for understanding fundamental issues, such as
the role of the boundary conditions, of geometric symme-
try and of the occurrence of reversible behavior. We have
left aside physical effects, in particular, capillarity, that
could add further functionalities, such as trapping in ta-
pered channels, splitting and merging of droplets at junc-

tions, etc. However, we believe, that the presented method
will stimulate further experiments to explore the validity of
its central ideas. After such a validation step it will provide
a guide for the design of devices, and for exploration of
new functionalities. In particular, it lends its ideas to *robust*
passive solutions that are likely steps for droplet (or bub-
ble) microfluidics to practically come up to the hopes it has
raised in many fields.

[1] T. Thorsen, R. W. Roberts, F. H. Arnold, and S. R. Quake,
Phys. Rev. Lett. **86**, 4163 (2001).
[2] Special issue, Lab Chip **4**, 31N (2004); M. Joanicot and
A. Ajdari, Science **309**, 887 (2005); J. L. Steinbacher and
D. T. McQuade, J. Polym. Sci., Part A: Polym. Chem. **44**,
6505 (2006); H. Song, D. L. Chen, and R. F. Ismagilov,
Angew. Chem., Int. Ed. **45**, 7336 (2006).
[3] A. Günther and K. F. Jensen, Lab Chip **6**, 1487 (2006).
[4] H. Song, J. D. Tice, and R. F. Ismagilov, Angew. Chem.,
Int. Ed. **42**, 768 (2003).
[5] B. Zheng and R. F. Ismagilov, Angew. Chem., Int. Ed. **44**,
2520 (2005).
[6] G. R. Yi *et al.*, Adv. Mater. **15**, 1300 (2003); D. Dendukuri,
K. Tsoi, T. A. Hatton, and P. S. Doyle, Langmuir **21**, 2113
(2005); T. Nisisako, T. Torii, T. Takahashi, and Y.
Takizawa, Adv. Mater. **18**, 1152 (2006).
[7] M. Prakash and N. Gershenfeld, Science **315**, 832 (2007).
[8] M. J. Fuerstman, P. Garstecki, and G. M. Whitesides,
Science **315**, 828 (2007).
[9] H. Willaime, V. Barbier, L. Kloul, S. Maine, and P.
Tabeling, Phys. Rev. Lett. **96**, 054501 (2006).
[10] P. Garstecki, M. J. Fuerstman, and G. M. Whitesides,
Nature Phys. **1**, 168 (2005).
[11] W. Engl, M. Roche, A. Colin, P. Panizza, and A. Ajdari,
Phys. Rev. Lett. **95**, 208304 (2005).
[12] G. Cristobal, J.-P. Benoit, M. Joanicot, and A. Ajdari,
Appl. Phys. Lett. **89**, 034104 (2006).
[13] F. Jousse, R. Farr, D. R. Link, M. J. Fuerstman, and P.
Garstecki, Phys. Rev. E **74**, 036311 (2006); F. Jousse *et al.*,
Lab Chip **5**, 646 (2005).
[14] F. P. Bretherton, J. Fluid Mech. **10**, 166 (1961).
[15] We believe that the parameters in Fig. 2(b) correspond to
the experimental conditions used by Fuerstman *et al.* [8].
The cascade of forward periods in their Fig. 2(b) indicates
an estimated value $L_d/\bar{L}_\ell \approx 1.5$, where we find a similar
cascade. Their forward train had a period of 7 which we
find in the interval $\lambda/\lambda_{max} \in [0.3646, 0.3837]$.
[16] In the special case of a single pair of end nodes (e.g., the
loop) the boundary conditions do not affect the sequence
of events but only the pace at which they occur.
[17] International Patent No. WO/2006/134274.